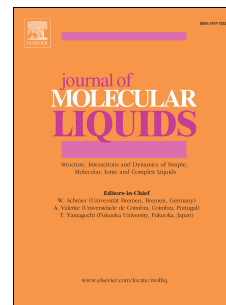


Journal Pre-proof

Measurement and correlation of liquid - Liquid equilibria of three imidazolium ionic liquids with acetone and cyclohexane

Zhaoyou Zhu, Ying Xu, Taixi Feng, Ningning Wang, Kai Liu, Haowen Fan, Juan A. Reyes-Labarta, Yinglong Wang, Jun Gao, Longlong Wang



PII: S0167-7322(19)34588-X

DOI: <https://doi.org/10.1016/j.molliq.2019.111947>

Reference: MOLLIQ 111947

To appear in: *Journal of Molecular Liquids*

Received Date: 15 August 2019

Revised Date: 13 October 2019

Accepted Date: 16 October 2019

Please cite this article as: Z. Zhu, Y. Xu, T. Feng, N. Wang, K. Liu, H. Fan, J.A. Reyes-Labarta, Y. Wang, J. Gao, L. Wang, Measurement and correlation of liquid - Liquid equilibria of three imidazolium ionic liquids with acetone and cyclohexane, *Journal of Molecular Liquids* (2019), doi: <https://doi.org/10.1016/j.molliq.2019.111947>.

This is a PDF file of an article that has undergone enhancements after acceptance, such as the addition of a cover page and metadata, and formatting for readability, but it is not yet the definitive version of record. This version will undergo additional copyediting, typesetting and review before it is published in its final form, but we are providing this version to give early visibility of the article. Please note that, during the production process, errors may be discovered which could affect the content, and all legal disclaimers that apply to the journal pertain.

© 2019 Published by Elsevier B.V.

Measurement and correlation of liquid - liquid equilibria of three imidazolium ionic liquids with acetone and cyclohexane

Zhaoyou Zhu^{a,d}, Ying Xu^a, Taixi Feng^a, Ningning Wang^a, Kai Liu^a, Haowen Fan^a, Juan A. Reyes-Labarta^e, Yinglong Wang^{a,d,*}, Jun Gao^b, Longlong Wang^c

^a*College of Chemical Engineering, Qingdao University of Science and Technology, Qingdao 266042, China*

^b*College of Chemical and Environmental Engineering, Shandong University of Science and Technology, Qingdao, 266590, China*

^c*Qingdao Hailin Water Group CO., LTD., Qingdao, 266102, China*

^d*Shandong Collaborative Innovation Center of Eco-Chemical Engineering, Qingdao University of Science and Technology, Qingdao, 266042, China*

^e*Chemical Engineering Department, University of Alicante, 03080 Alicante, Spain*

Corresponding Author

*E-mail: wangyinglong@qust.edu.cn

Abstract: Ionic liquids (ILs) can be recycled as extractants for their low vapor pressure and volatility. More and more applications are applied to the separation of industrial organic matter. The industrial production of ILs has gradually been realized, which also widens the way for the application of ILs. In this work, the liquid-liquid extraction of cyclohexane-acetone azeotropic mixture with different ILs {1-butyl-3-methylimidazolium bis(trifluoromethylsulfonyl), 1-butyl-3-methylimidazolium trifluoromethanesulfonate and 1-butyl-3-methylimidazolium dicyanamide} is studied. The extraction mechanism is discussed based on the molecular scale. The relationship between hydrogen bond donor and acceptor between ILs and acetone is analyzed by COSMO-SAC. The interaction between molecules is optimized and calculated by Materials Studio 7.0. The extraction ability of ILs is analyzed by radial distribution function, and the experimental results are verified. The liquid-liquid equilibrium test is carried out at 298.15K. Distribution and selectivity are indices used to judge the extraction efficiency of ILs. The NRTL model and UNIQUAC model are adopted to correlate the liquid-liquid equilibrium data. The results show that all of the two models can well correlate the experimental.

Keywords: Liquid-liquid equilibrium; Molecular scale; Radial distribution function; Ionic liquids; Binary interaction parameters; Thermodynamic models

1. Introduction

Acetone is an important chemical raw material which is used in the manufacture of bisphenol A, acetone cyanohydrin, hexanediol, etc [1-2]. Cyclohexane can be used as solvent of rubber, paint and varnish, diluent of adhesives and oil extractant [3]. The binary mixtures of acetone and cyclohexane can be used as mixed solvents [4-6], synthetic raw materials, or entrainers for supercritical fluid dissolution [7], and play an important role in chemical production and scientific research. In order to reduce the cost, it is hoped that the mixture of acetone and cyclohexane can be separated and recycled, but they form azeotropic system and can not be separated by conventional distillation. At present, for the separation of azeotropic systems, the main methods are adsorption, azeotropic distillation [8, 9], extractive distillation [10, 11], reactive distillation, salt-adding distillation, membrane separation, pressure-swing distillation [12, 13]. In addition, liquid-liquid extraction [14-16] is a widely used azeotrope separation method. Ionic liquids (ILs) are of great interest and potential in the liquid-liquid extraction due to their excellent properties, such as low vapor pressure, non-flammability and chemical/thermal stability, which make them to a favorable solvent compared to traditional organic solvents [17-21]. ILs also can simplify the solvent recovery process and achieve separation from other substances through flash evaporation [22-24].

For the separation of different compounds, several potential mechanisms have been proposed to explain the separation process. For example, Cassandra et al. [25] reported the free energy of solubility calculated by conductor shielding model (COSMO-RS) is tallies well with the experimental results. Li et al. [26] used a DFT method to visually analyze the interaction properties. Wang et al. [27] believed that molecular dynamics is an effective tool to study LLE in mixtures containing polar and non-polar components.

The extraction ability of ILs can be judged by calculating the interaction energy. The absolute value of interaction energy is positively correlated with the extraction ability of ILs. [28, 29] Then the extraction efficiency of acetone in the selected ILs is analyzed by using the radial distribution function (RDF). The calculated RDF diagram shows that the higher the peak value is positively correlated with the extraction effect of ILs. [30-32] The mechanism of the separation process

reveals the form and intensity of the interaction between ILs and acetone, which can guide the selection of subsequent extractants. Therefore, in this work, the mechanism of extraction is analyzed on the molecular scale. To explain the extraction theory between ILs and acetone, the relationship between donor and receptor of hydrogenation bond is verified by COSMO-SAC model. In addition, the possible interactions between molecules are confirmed by the bond length, interaction energy and electron density between the selected ILs and acetone. Then, the extraction efficiency of acetone from selected ILs are analyzed by using RDF. At the same time, to separate acetone-cyclohexane azeotropic mixture with ILs as extractant, the ternary LLE data are measured at 298.15 K for systems of {cyclohexane + acetone + 1-butyl-3-methylimidazolium bis(trifluoromethylsulfonyl), [BMIM][OTf], cyclohexane + acetone + 1-butyl-3-methylimidazolium trifluoromethanesulfonate, [BMIM][NTf₂], cyclohexane + acetone + 1-butyl-3-methylimidazolium dicyanamide, [BMIM][N(CN)₂]}. Then, β and S are obtained on the basis of the experimental data. Finally, the thermodynamic model NRTL and UNIQUAC are used to correlate the phase equilibrium data and the corresponding binary interaction parameters are obtained.

2. Molecular scale analysis

Abraham et al. [33] and Mali et al. [34] analyzed the effect of hydrogen bond on the extraction process of ILs and extracts. Therefore, after understanding the extraction mechanism, it is helpful to screen a series of ILs, which could be used to separate acetone from cyclohexane.

2.1. COSMO-SAC model and σ -profiles analysis

Klamt et al. [35] proposed the COSMO approach which allows for the calculation of a relatively simple, specific expression for the selecting energy of a molecule in a dielectric medium. In addition, Sandler et al. [36] propose a conductor-like shielding model with fragment activity coefficient (COSMO-SAC) to calculate the properties of various substances including ILs. This model is similar to COSMO-RS model and can be used to calculate the thermodynamic properties of the system. Because of the superiority of COSMO model, many quantum chemical calculation software (Gaussian, TURBOMOLE, GAMESS and Material Studio) have COSMO calculation methods. At the same time, COSMO-SAC model has been extensively applied in the calculation of thermodynamic data of ILs systems [37-40].

Firstly, we get the molecular structure from the database (Scifinder, ChemSpider, and NIST database) and load the molecular structure in the Materials Studio 7.0. Secondly, based on DMOL³ module and DFT theory, the initial molecules structure are optimized. Among them, GGA/VWN-BP functional function is used. The actual space truncation value is set to 5.5 Å and the basic setting is DNP 4.4. Finally, each molecule forms COSMO files on the basis of geometric optimization. Meanwhile, the COSMO data of the selected ILs and acetone are imported into origin to obtain the σ -profile. The σ -profile of cyclohexane, acetone and ILs are shown in Figure 1. In Figure 1, the σ -profile is separated into three areas by two perpendicular lines ($\sigma = \pm 0.0082 \text{ e}/\text{Å}^{-2}$). The middle part of $-0.0082 \text{ e}/\text{Å}^{-2} < \sigma < + 0.0082 \text{ e}/\text{Å}^{-2}$ is the nonhydrogen bond region. The left side of $\sigma < -0.0082 \text{ e}/\text{Å}^{-2}$ is the hydrogen bond donor region. The right side of $\sigma > + 0.0082 \text{ e}/\text{Å}^{-2}$ is the hydrogen bond acceptor region.

Surface charge distribution of a molecule can be reflected by the σ -profile. According to the distribution region of the molecule in the σ -profile, the ability of acceptance or supply of hydrogen bond can be judged. By analyzing the supply or acceptance of hydrogen bonds by ILs, cyclohexane and acetone, it can be concluded that the extracted substances who are easier to form hydrogen bonds with ILs. In Fig. 1, [BMIM]NTF₂, [BMIM]OTF and [BMIM]N(CN)₂ exist in the range of $[-0.015, 0.011] \text{ e}/\text{Å}^{-2}$, $[-0.011, 0.008] \text{ e}/\text{Å}^{-2}$ and $[-0.015, 0.010] \text{ e}/\text{Å}^{-2}$, which illustrates intense polarity at the regional of hydrogen donor. Cyclohexane are distributed from the scope of $[-0.015, 0.006] \text{ e}/\text{Å}^{-2}$ which illustrate intense polarity at the regional of hydrogen donor. Acetone is distributed within the scope of $[-0.007, 0.015] \text{ e}/\text{Å}^{-2}$ which illustrates intense polarity at the regional of hydrogen acceptor. Therefore, ILs are more likely to form hydrogen bonds with acetone.

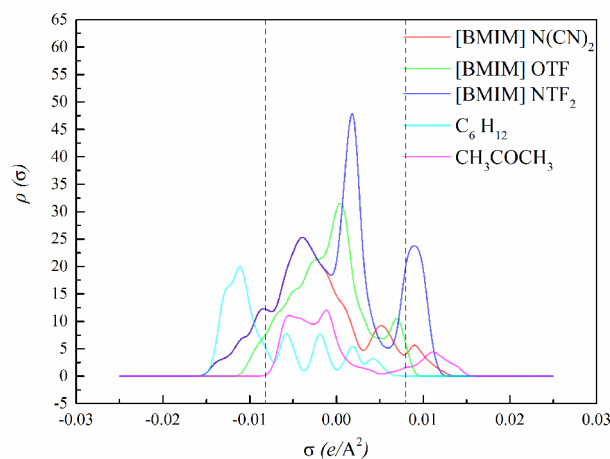


Fig. 1. σ -Profiles for cyclohexane, acetone and different anions.

2.2. Quantum chemical calculations

The interaction between molecules is discussed based on the optimization of geometric configuration. Above, the donor-acceptor relationship of hydrogen bond can be gained by analyzing σ -profile. The analysis shows that acetone may form hydrogen bonds with selected ILs, so, the bond length, interaction energies and electron density analysis between selected ILs and acetone are analyzed to check above hypothesis. The calculation is divided into two steps.

Firstly, the correct molecular structure is introduced into the Material Studio 7.0. and optimized in the Dmol³ module. The parameter settings are the same as above. It is important to note that all structures must be the minimal energy in the global. All the molecules used in this paper must be optimized separately, and next the combined structures will be optimized again.

After structural optimization, it can be seen from Fig. 2-4. that the atomic distance between oxygen atoms of acetone and hydrogen atom on a cation in ILs is less than the total of its van der Waals's radii. The distances between atoms are 2.047, 2.020 and 2.084.

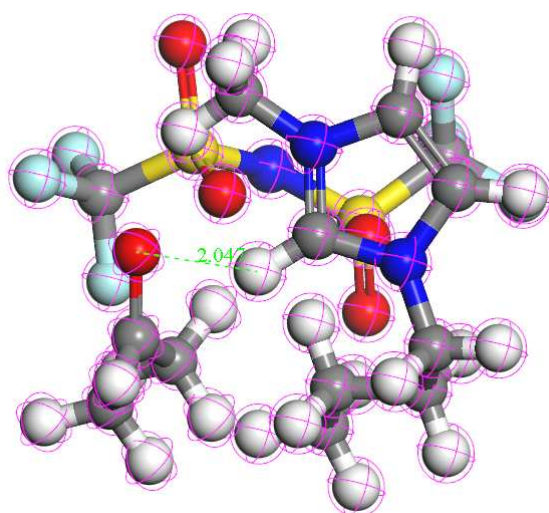


Fig. 2. Hydrogen bonding length for [BMIM][NTF₂] with acetone.

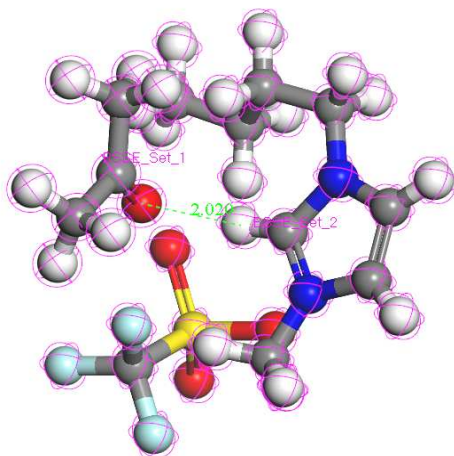


Fig. 3. Hydrogen bonding length for [BMIM][OTF] with acetone.

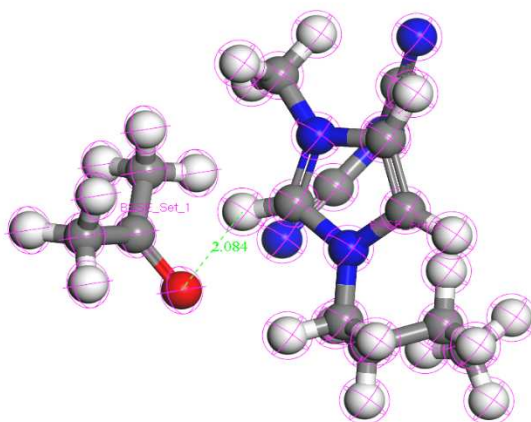


Fig. 4. Hydrogen bonding length for [BMIM][N(CN)₂] with acetone.

Secondly, the interaction energy is calculated in detail. After geometric optimization of

monomer or complex ligand, the energy calculation is carried out by this method. In order to make the results more accurate, the base set superposition error (BSSE) is corrected by the balanced correction method [41]. The calculation formula is as follows:

$$\Delta E = E_{AB} - E_A - E_B + E_{BEES} \quad (1)$$

$$E_{BEES} = E_A - E_{(A,AB)} + E_B - E_{(B,AB)}, \quad (2)$$

where E_{AB} is the intermolecular interaction energy of A and B, E_A and E_B are the energy of molecule A(ILs) and B(acetone). $E_{(B,AB)}$ represents the energies of A in the A, B. The explanation of $E_{(B,AB)}$ is as mentioned above. The results of calculation are presented in Table 1. The calculated energies for acetone + [BMIM]NTF₂/[BMIM]OTF/[BMIM]N(CN)₂ are -73.581476kJ·mol⁻¹, -56.847552kJ·mol⁻¹ and -32.535705kJ·mol⁻¹. This result indicates that there is a strong interaction between acetone and selected ILs. The order of interaction energy is [BMIM]NTF₂ > [BMIM]OTF > [BMIM]N(CN)₂.

The charge density between the selected ILs and acetone can be utilized for defining the formation of hydrogen bonds. Furthermore, the sum of electron density for ILs and acetone are shown in Fig. 5-7. The C-H···O interaction between the cation of [BMIM]NTF₂/[BMIM]OTF/[BMIM]N(CN)₂ and acetone are apparent when the isovalue is 0.14, 0.15 and 0.14.

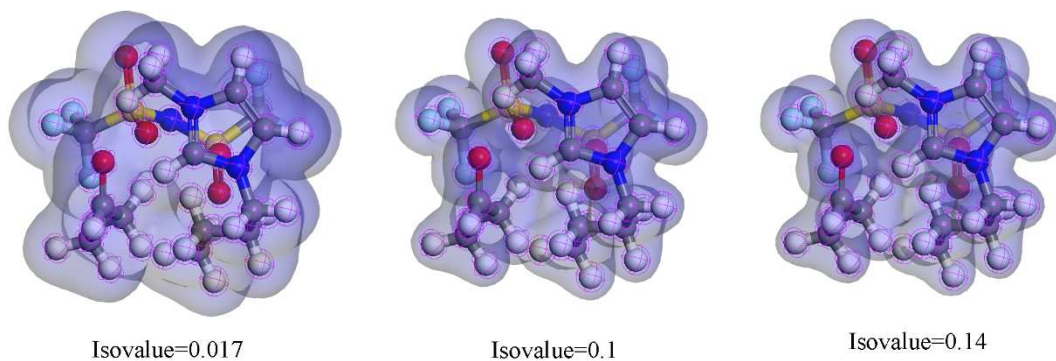


Fig. 5. Total density maps of different isovalues for [BMIM][NTF₂] with acetone.

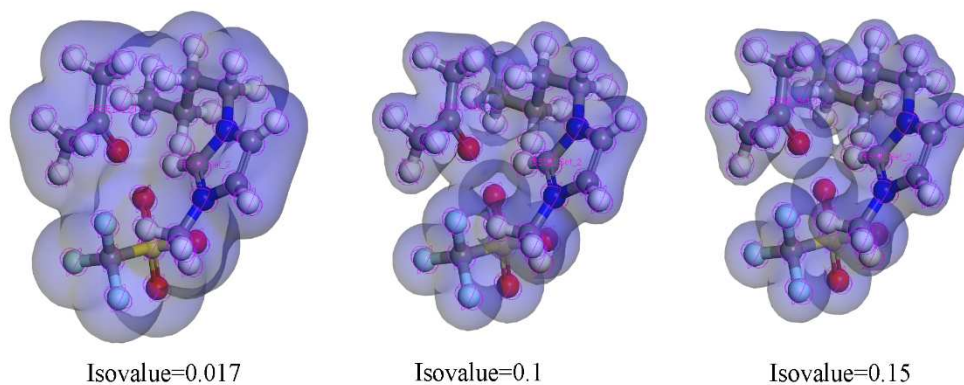


Fig. 6. Total density maps of different isovalues for [BMIM][OTF] with acetone.

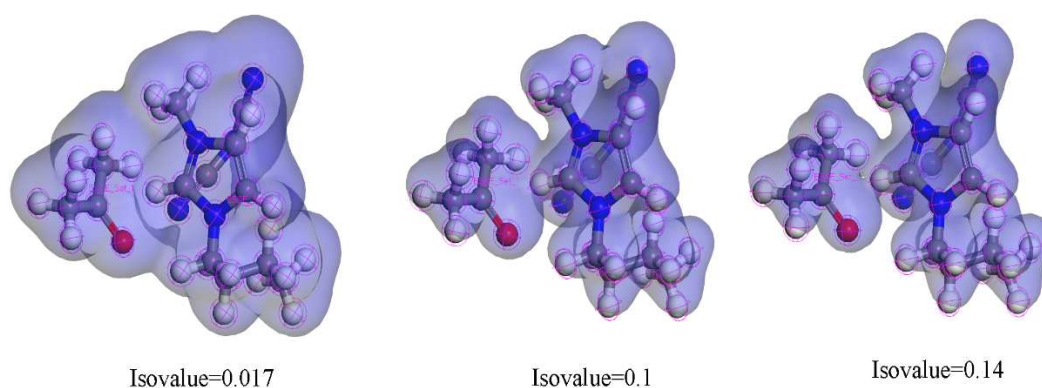


Fig. 7. Total density maps of different isovalues for [BMIM][N(CN)₂] with acetone.

On the side, deformed electron density for selected ILs and acetone are shown in Fig. 8-10. Figure 8-10 shows a cross section of the deformation density, which illustrates that the C-H...O bonding interaction is easy to be determined. The bonding effect between the O atoms and H atoms in selected ILs in acetone is shown, which the region of receiving electrons around O atom is red, and the area of losing electrons surrounding H atom is blue.

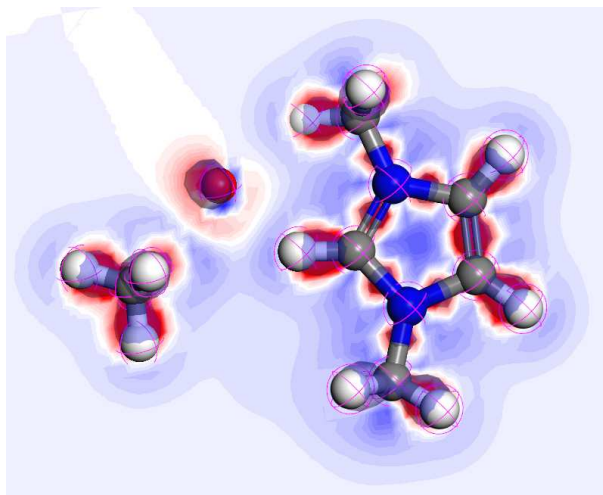


Fig. 8. Deformation charge density maps for [BMIM][NTF₂] with acetone.

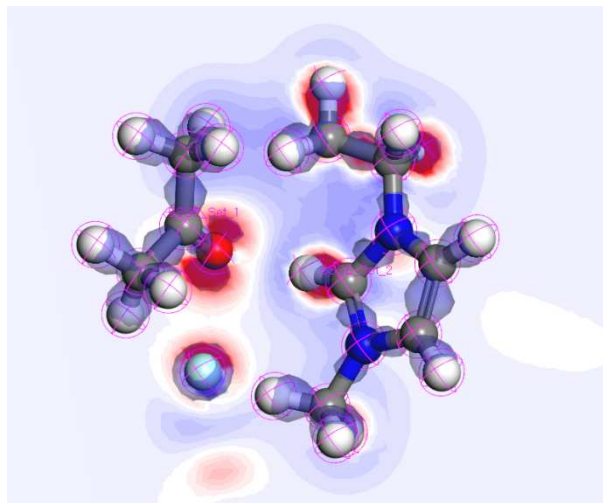


Fig. 9. Deformation charge density maps for [BMIM][OTF] with acetone.

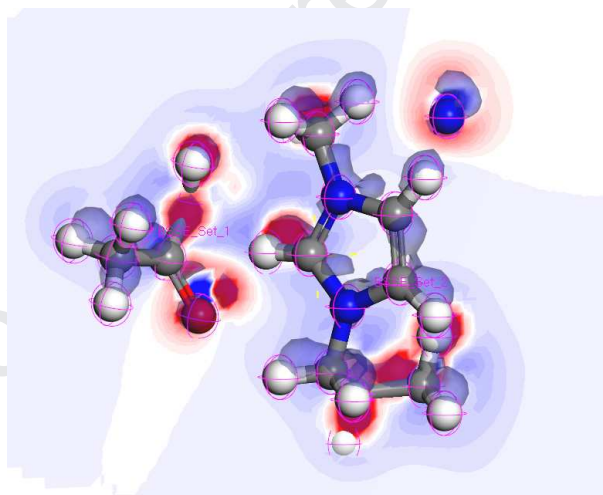


Fig. 10. Deformation charge density maps for [BMIM][N(CN)₂] with acetone.

2.3. Simulation methods

Firstly, the molecular structures of selected ILs and acetone are downloaded from Chemical Book. Then, the partial charges of all molecules are obtained by the charge derivation method of restraining electrostatic potential [42, 43]. Generalized Amber Force Field functional modality is applied to shape the force field parameters of the compounds by ANTECHAMBER module [44, 45].

In order to understand the structure of acetone in ILs, molecular dynamics simulation of ILs-acetone mixture is applied. At constant temperature (298.15 K) and 1 atm pressure,

GROMACS2018.432 software is used by Langevin thermostat and Nose-Hoover Langevin barostat [46, 47]. In order to deal with the long-range electrostatic interactions, the nonbonded LJ interactions are cut off at 12\AA by applying long range tail corrections. All the initial simulation boxes are built using Packmol35 software. The dimension of the simulation box is about $3.0 \times 3.0 \times 3.0 \text{ nm}^3$ and it is made up of 100 acetone and 300 ILs. Solution-solvent interaction is described by OPLS atomic force field. At 293.15K and 1 bar, the energy of the system is minimized by preliminary simulation of 50000. Then, the system is gradually heated to 298.15K and lasts for 3ns in NVT ensemble. After reaching the expected temperature, the subsequent equilibrium is applied in NPT ensemble, lasting for 30ns. The following result is analyzed according to the trajectories obtained within the last 30ns NPT production operation. To obtain insight into the relationship between the acetone and different ILs, center-of-mass radial distribution functions (RDF) of the different ILs is derived from the MD trajectories, as shown in Fig. 11. The center of mass RDF has been computed using Visual Molecular Dynamics (VMD). In Fig. 11, the RDF of the acetone with different ILs shows peak height in the sequence of $[\text{BMIM}]\text{NTF}_2 > [\text{BMIM}]\text{OTF} > [\text{BMIM}]\text{N}(\text{CN})_2$, which shows the strength of the interaction. This shows the extraction effect is $[\text{BMIM}]\text{NTF}_2 > [\text{BMIM}]\text{OTF} > [\text{BMIM}]\text{N}(\text{CN})_2$.

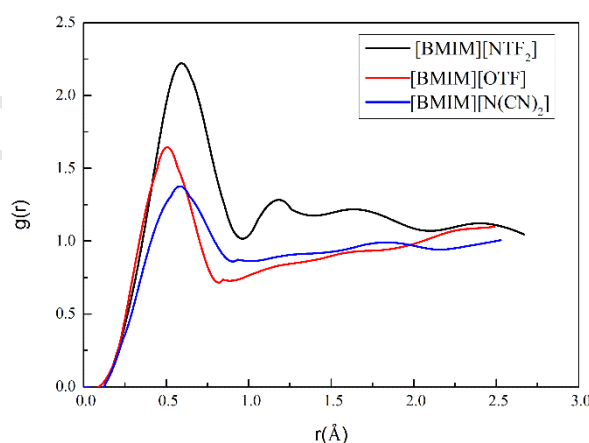


Fig. 11. Radial distribution functions of ILs and acetone.

3. Experiment

After the above mechanism analysis, the result shows the extraction effect is $[\text{BMIM}]\text{NTF}_2 > [\text{BMIM}]\text{OTF} > [\text{BMIM}]\text{N}(\text{CN})_2$. Then, the LLE experiment is carried out to verify the analysis

results.

3.1. Chemicals

Cyclohexane with 99.5% mass fraction and ethanol with 99.8% mass fraction are purchased from Tianjin Kermel Chemical Reagent Co., Ltd., and acetone with 99.5% mass fraction is purchased from Yantai Far East Fine Chemical Co., Ltd. The purity of all the reagents used in the experiment is determined by gas chromatography (GC-2014C). All chemicals are directly used without further purification. All chemical structures, CAS numbers and other details are shown in Table 2.

3.2. Apparatus and procedure

The LLE for three ternary systems of {cyclohexane + acetone + [BMIM][OTf], cyclohexane + acetone + [BMIM][NTF₂], cyclohexane + acetone + [BMIM][N(CN)₂]} are measured at 298.15 K and 101.325 kPa. Relevant measuring procedure and equipment can be searched for in our previous work [48, 49]. The cyclohexane, acetone and the ILs are mixed into a mixture according to different mass ratios, and the mixture is placed in a self-designed equilibrium cell. The mixture is stirred vigorously for three hours with a stir bar of approximately 1000 r/min. The mixture is placed for about 15 hours and completely separated. In the process of mixing and standing, a cryostat (accurate to 0.05 K) is used to keep the temperature at 298.15 K. After a period of stationary time, the mixture is stratified.

The gas chromatography (GC) packed column with Porapak Q column and thermal conductivity detector (TCD) was prepared. The carrier gas was helium with purity over 99.99%. In this experiment, ethanol is used as internal standard. The contents of acetone, cyclohexane and ethanol in the samples are determined by GC. Each sample should be analyzed at least three times. For ILs, the quality difference method is used to analyze the composition. The components of ILs were analyzed by mass difference method, due to ILs could not be detected by GC. Then samples were placed in a vacuum drying chamber with a temperature of 408.15 K for 48 hours.

4. Results and discussion

4.1. Experimental results

The LLE data of cyclohexane (1) + acetone (2) + ILs (3) system at 298.15 K were determined. The results were shown in Table 3. Fig. 12-14 shows the contact tie-line of ternary

systems. When equilibrium is reached, the two liquid layers are called conjugated phases, and the line connecting the coordinates of the conjugated liquid phase is called the conjugated line. The extraction operation can only be carried out in the two-phase region, i.e. within the solubility curve. The three-phase diagram in this manuscript has a large immiscible region. From the three-phase diagram, the liquid-liquid extraction range of each system was wide and the selected ILs were suitable for the extraction of cyclohexane + acetone mixture.

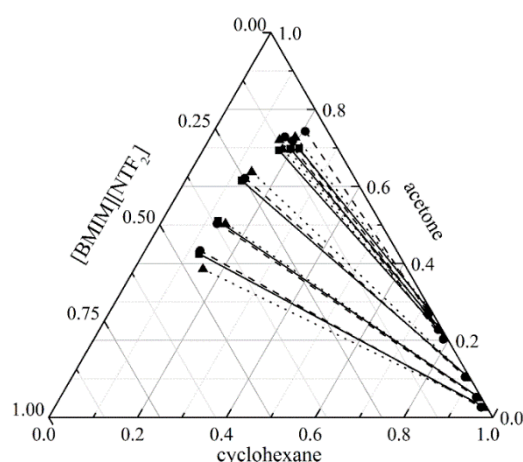


Fig 12. Experimental and calculated LLE data in mole fraction for the system of cyclohexane (1) + acetone (2) + [BMIM][NTf2] (3) at 298.15 K. (■), experimental value; (●), calculated value by NRTL model; (▲), calculated value by UNIQUAC model.

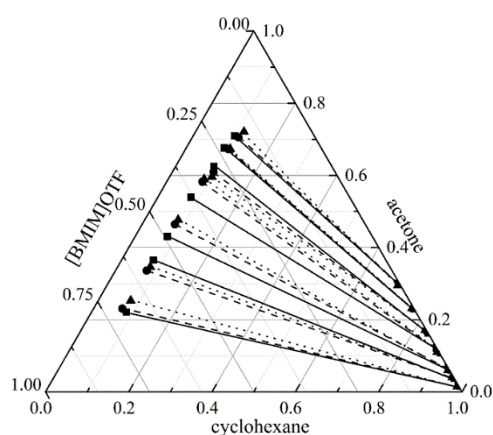


Fig 13. Experimental and calculated LLE data in mole fraction for the system of cyclohexane (1) + acetone (2) + [BMIM][OTF] (3) at 298.15 K. (■), experimental value; (●), calculated value by NRTL model; (▲), calculated value by UNIQUAC model.

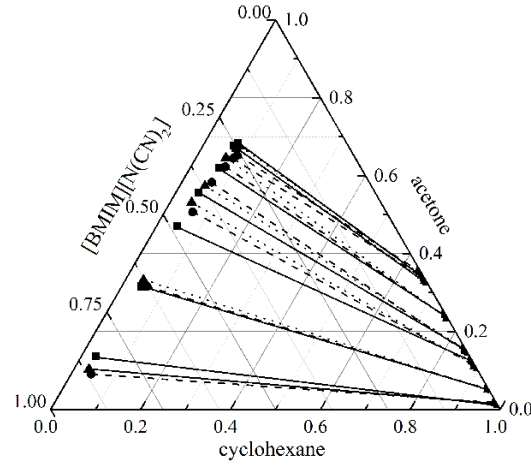


Fig. 14. Experimental and calculated LLE data in mole fraction for the system of cyclohexane (1) + acetone (2) + [BMIM][N(CN)2] (3) at 298.15 K. (■), experimental value; (●), calculated value by NRTL model; (▲), calculated value by UNIQUAC model.

In the process of liquid-liquid extraction, distribution coefficient (β) and separation factor (S) are important parameters for evaluating solvent separation performance. β and S show in Fig.15 and Fig. 16. Formula β [50] and S [51] is defined as follows.

$$\beta = \frac{\chi_2^{IL-rich}}{\chi_2^{cyclohexane-rich}} \quad (3)$$

$$S = \frac{(\chi_2^{IL-rich} / \chi_1^{IL-rich})}{(\chi_2^{cyclohexane-rich} / \chi_1^{cyclohexane-rich})} \quad (4)$$

Where χ represents the mole fraction and subscript 1 represents cyclohexane subscript 2 represents acetone. The superscript cyclohexane-rich indicates the cyclohexane enrichment phase and the IL-rich indicates the ILs enrichment phase.

The calculated β and S values for the ternary system (cyclohexane-acetone-ILs) were shown in Table 3. The calculated value of β is greater than 1, which indicates that all ILs can extract acetone from cyclohexane effectively.

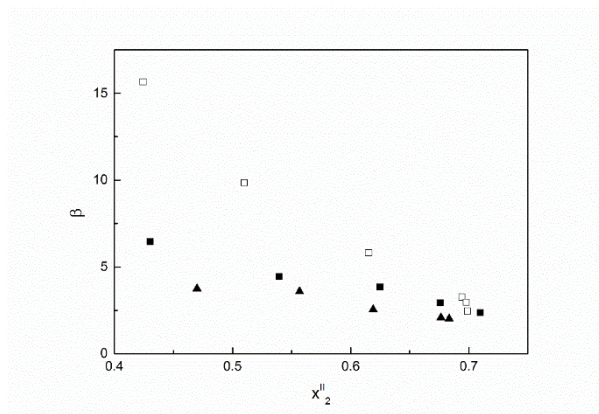


Fig. 15. Distribution coefficient (β) for ternary systems of cyclohexane + acetone + ILs, x_2^{II} is the mole fraction of acetone in ILs-rich phase. (\square), cyclohexane + acetone + [BMIM][NTF₂] at 298.15 K; (\blacksquare), cyclohexane + acetone + [BMIM][OTF] at 298.15 K; (\blacktriangle), cyclohexane + acetone + [BMIM][N(CN)₂] at 298.15 K.

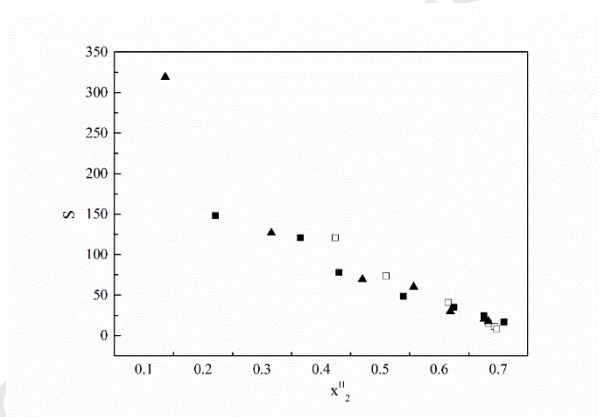


Fig. 16. Separation factor (S) for ternary systems of cyclohexane + acetone + ILs, x_2^{II} is the mole fraction of acetone in ILs-rich phase. (\square), cyclohexane + acetone + [BMIM][NTF₂] at 298.15 K; (\blacksquare), cyclohexane + acetone + [BMIM][OTF] at 298.15 K; (\blacktriangle), cyclohexane + acetone + [BMIM][N(CN)₂] at 298.15 K.

4.2. LLE correlation

The experimental data shown in Table 3 are correlated with NRTL and UNIQUAC models. Using the non-linear least squares method (programmed in MATLAB), the binary interaction parameters of NRTL and UNIQUAC models are determined by data regression in Table 3. The r and q values of UNIQUAC model are obtained by consulting literatures and the values are shown in Table 5. The molecular interaction is studied in a system of {cyclohexane + acetone +

[BMIM][NTF₂], cyclohexane + acetone + [BMIM][OTF] and cyclohexane + acetone + [BMIM][N(CN)₂]. The liquid–liquid phase equilibrium [52] is expressed as follows :

$$\lambda_i^I x_i^I = \lambda_i^{II} x_i^{II} \quad (5)$$

where χ_i^I is the mole fraction of component i in the organic rich layer, χ_i^{II} is the mole fraction of component i in the IL rich layer, λ_i^I , and λ_i^{II} are the activity coefficients of component i in the different layer.

The binary interaction parameters (Δg_{ij}) and non-randomness factor (α) are used for the NRTL model, and the binary interaction parameters (Δu_{ij}) are used for UNIQUAC model. The binary interaction parameters of the NRTL and UNIQUAC are regressed by minimizing the value of the objective function (OF). The root mean square deviation ($rmsd$) determines the calculated value. The equations of the OF [53] and $rmsd$ [54] are as follows:

$$OF = \sum_{k=1}^M \sum_{j=1}^2 \sum_{i=1}^3 (x_{ijk}^{exp} - x_{ijk}^{calc})^2 \quad (6)$$

$$rmsd = 100 \left(\frac{\sum_{k=1}^M \sum_{j=1}^2 \sum_{i=1}^3 (x_{ijk}^{exp} - x_{ijk}^{calc})^2}{6M} \right)^{1/2} \quad (7)$$

Where M represents the number of tie-lines, subscripts *exp* and *calc* represent the experimental data of each component and calculated values, and subscripts *i*, *j*, and *k* represent the component, phase, and tie-line. In Fig. 12-14, the connection line data between the two models and the experiments in three ternary systems are represented in three-phase diagrams. The $rmsd$ of NRTL and UNIQUAC are given in Table 4.

5. Conclusions

In this paper, the extraction process of acetone from cyclohexane is studied by using quantum chemical calculation, RDF and phase equilibrium verification. For determining the interaction between molecules and separation ability, multi-scale simulation of extraction process is carried out. The donor-acceptor relationship of hydrogen bond is analyzed by σ -Profiles. At the same time, the C-H...O hydrogen bond between the selected ILs and acetone is certificated on the strength of the Dmol³ module calculations. The interaction energy between different ILs and acetone are calculated. The larger the absolute value of the interaction energy is, the stronger the interaction is,

and the better the extraction effect of ILs on acetone is. The order of interaction energy is $[\text{BMIM}]\text{NTF}_2 > [\text{BMIM}]\text{OTF} > [\text{BMIM}]\text{N}(\text{CN})_2$. According to the calculated RDF graph, the higher the peak is, the better the extraction effect of ILs is. The extraction effect is $[\text{BMIM}]\text{NTF}_2 > [\text{BMIM}]\text{OTF} > [\text{BMIM}]\text{N}(\text{CN})_2$. Meanwhile, the experimental LLE data is determined by measuring the cyclohexane + acetone + ILs ternary system at 298.15 K and 1 bar, systems of cyclohexane + acetone + $[\text{BMIM}][\text{NTF}_2]$, $[\text{BMIM}][\text{OTF}]$, and $[\text{BMIM}][\text{N}(\text{CN})_2]$ show great separation effect. The experimental results are shown in Table 3. β and S are important parameters for evaluating solvent separation performance. According to the experimental results, the extraction capacity is $[\text{BMIM}]\text{NTF}_2 > [\text{BMIM}]\text{OTF} > [\text{BMIM}]\text{N}(\text{CN})_2$. These results are in good agreement with the experimental result. Therefore, these three studies have investigated that ILs are suitable solvents for acetone purification. Finally, NRTL and UNIQUAC models are used to verify the accuracy of the experiment.

Acknowledgement

This work is supported by the National Natural Science Foundation of China (No. 21776145), National Natural Science Foundation of China (No. 21676152).

Reference

- [1] W. Rahmaliaa, J. Fabre, Z. Mouloungui, Effects of Cyclohexane/Acetone Ratio on Bixin Extraction Yield by Accelerated Solvent Extraction Method, *Procedia Chemistry*. 14 (2015) 455-464.
- [2] C. C. Bannan, G. Calabró, D. Y. Kyu, D. L. Mobley, Calculating Partition Coefficients of Small Molecules in Octanol / Water and Cyclohexane/Water, *Theory Comput*. 12 (2016) 4015-4024.
- [3] S. Ma, J. li, L. li, et al. Liquid–Liquid Extraction of Benzene and Cyclohexane Using Sulfolane-Based Low Transition Temperature Mixtures as Solvents: Experiments and Simulation, *Energy & fuels*. 32 (2018) 8006-8015.
- [4] W. Rahmalia, J. F. Fabre, Z. Mouloungui, Effects of cyclohexane/acetone ratio on bixin extraction yield by accelerated solvent extraction method, *Procedia Chemistry*. 14 (2015) 455-464.
- [5] A. A. Ksenofontov, G. B. Guseva, S. A. Stupikova, E. V. Antina, Novel Zinc (II) Bis (Dipyrromethenate)-Doped Ethyl Cellulose Sensors for Acetone Vapor Fluorescence Detection, *Journal of fluorescence*. 28 (2018) 477-482.
- [6] E. Mourad, O. Fontaine, Redox bucky gels: mixture of carbon nanotubes and room temperature redox ionic liquids, *Journal of Materials Chemistry A*. 7 (2019) 13382-13388.
- [7] D. L. Gurina, M. L. Antipova, E. G. Odintsova, V. E. Peterenko, The study of peculiarities of parabens solvation in methanol- and acetone-modified supercritical carbon dioxide by computer simulation, *The Journal of Supercritical Fluids*. 126 (2017) 47-54.
- [8] Q. K. Le, I. J. Halvorsen, O. Pajalic, S. Skogestad, Dividing wall columns for heterogeneous azeotropic distillation, *Chemical Engineering Research and Design*. 99 (2015) 111-119.
- [9] Y. Wang, X. Zhang, X. Liu, W. Bai, Z. Zhu, Y. Wang, J. Gao, Control of extractive distillation process for separating heterogenous ternary azeotropic mixture via adjusting the solvent content, *Separation and Purification Technology*. 191 (2018) 8-26.
- [10] Y. C. Chen, B. Y. Yu, C. C. Hsu, I. L. Chien, Comparison of heteroazeotropic and extractive distillation for the dehydration of propylene glycol methyl ether, *Chemical Engineering Research and Design*. 111(2016) 184-195.
- [11] Y. Zhao, K. Ma, W. Bai, D. Du, Z. Zhu, Y. Wang, J. Gao, Energy-saving thermally coupled

- ternary extractive distillation process by combining with mixed entrainer for separating ternary mixture containing bioethanol, *Energy*. 148 (2018) 296-308.
- [12] Q. Zhang, M. Liu, C. Li, A. Zeng, Heat-integrated pressure-swing distillation process for separating the minimum-boiling azeotrope ethyl-acetate and ethanol, *Separation and Purification Technology*. 189 (2017) 310-334.
- [13] B. Kiran, A. K. Jana, A hybrid heat integration scheme for bioethanol separation through pressure-swing distillation route, *Separation and Purification Technology*. 142 (2015) 307-315.
- [14] Q. Zeng, B. Hu, H. Cheng, L. Chen, J. Huang, Z. Qi, Liquid-liquid equilibrium for the system of ionic liquid [BMIm][HSO₄] catalysed isobutyl isobutyrate formation, *The Journal of Chemical Thermodynamics*. 122 (2018) 162-169.
- [15] S. Corderí, N. Calvar, E. Gomez, A. Domínguez, Capacity of ionic liquids [EMIm][NTf₂] and [EMpy][NTf₂] for extraction of toluene from mixtures with alkanes: comparative study of the effect of the cation, *Fluid Phase Equil.* 315 (2012) 46-52.
- [16] J. García, A. Fernandez, J.S. Torrecilla, M. Oliet, F. Rodríguez, Liquid-liquid equilibria for {hexane|benzene|1-ethyl-3-methylimidazolium ethylsulfate} at (298.2, 313.2 and 328.2) K, *Fluid Phase Equil.* 282 (2009) 117-120.
- [17] S. Zhang, C. Xu, X. Lv, Q. Zhou, *Ionic Liquids and Green Chemistry*, Science Press, Beijing, 2009.
- [18] Z. Zhang, K. Wu, Q. Zhang, T. Zhang, D. Zhang, R. Yang, W. Li, Separation of ethyl acetate and ethanol azeotrope mixture using dialkylphosphates-based ionic liquids as entrainers, *Fluid Phase Equilib.* 454 (2017) 91-98.
- [19] L. Alonso, A. Arce, M.a. Francisco, A. Soto, Extraction ability of nitrogen-containing compounds involved in the desulfurization of fuels by using ionic liquids, *J. Chem. Eng. Data* 55 (2010) 3262-3267.
- [20] M. Francisco, A. Arce, A. Soto, Ionic liquids on desulfurization of fuel oils, *Fluid Phase Equilib.* 294 (2010) 39-48.
- [21] M.C. Castro, A. Arce, A. Soto, H. Rodríguez, Liquid-liquid equilibria of mutually immiscible ionic liquids with a common anion of basic character, *J. Chem. Thermodyn.*

- 102 (2016) 12–21.
- [22] Q. Zeng, B. Hu, H. Cheng, L. Chen, J. Huang, Z. Qi, Liquid-liquid equilibrium for the system of ionic liquid [BMIm][HSO₄] catalysed isobutyl isobutyrate formation, *J. Chem. Thermodyn.* 122 (2018) 162-169.
- [23] M. Karpińska, U. Domańska, Liquid-liquid extraction of styrene from ethylbenzene using ionic liquids, *J. Chem. Thermodyn.* 124 (2018) 153-159.
- [24] M. Karpińska, M. Wlazło, M. Zawadzki, U. Domańska, Liquid-liquid separation of hexane / hex-1-ene and cyclohexane / cyclohexene by dicyanamide-based ionic liquids, *J. Chem. Thermodyn.* 116 (2018) 299-308.
- [25] C. Breil, M. A.Vian, T. Zemb, et al. “Bligh and Dyer” and Folch Methods for Solid-Liquid-Liquid Extraction of Lipids from Microorganisms. Comprehension of Solvation Mechanisms and towards Substitution with Alternative Solvents, *International journal of molecular sciences.* 18 (2017) 708.
- [26] H. Li, P. Zhou, J. Zhang, D. Li, X. Li, X. Gao, A theoretical guide for screening ionic liquid extractants applied in the separation of a binary alcohol-ester azeotrope through a DFT method, *Journal of Molecular Liquids.* 251 (2018) 51-60.
- [27] X. Wang, X. Gu, S. Murad, Molecular dynamics simulations of liquid-liquid phase equilibrium of ternary methanol/water/hydrocarbon mixtures, *Fluid Phase Equilibria.* 470 (2018) 109-119.
- [28] Ramalingam A. Interaction energy of pyrrole and pyridine with 1-ethyl-3-methylimidazolium ethyl sulphate. *Journal of Molecular Liquids.* 231(2017) 56-63.
- [29] Wang P, Xu D, Yan P, et al. Separation of azeotrope (ethanol and ethyl methyl carbonate) by different imidazolium-based ionic liquids: Ionic liquids interaction analysis and phase equilibrium measurements. *Journal of Molecular Liquids.* 261(2018) 89-95.
- [30] H. Gao, S. Zeng, X. Liu, et al. Extractive desulfurization of fuel using N-butylpyridinium-based ionic liquids[J], *RSC Advances.* 5 (2015) 30234-30238.
- [31] W. Zheng, L. Zheng, W. Sun, et al. Screening of imidazolium ionic liquids for the isobutane alkylation based on molecular dynamic simulation[J], *Chemical Engineering Science.* 183 (2018) 115-122.

- [32] E. G. Blanco-Díaz, E. O. Castrejón-González, J. F. JAlvarado, et al. Rheological behavior of ionic liquids: Analysis of the H-bond formation by molecular dynamics[J], *Journal of Molecular Liquids*. 242 (2017) 265-271.
- [33] M.H. Abraham, J.C. Dearden, G.M. Bresnen, Hydrogen bonding, steric effects and thermodynamics of partitioning, *J. Phys. Org. Chem.* 19 (2006) 242–248.
- [34] K.S. Mali, G.B. Dutt, T. Mukherjee, Do organic solutes experience specific interactions with ionic liquids? *J. Chem. Phys.* 123 (2005) 174504.
- [35] A. Klamt, G. Schüürmann, COSMO: a new approach to dielectric screening in solvents with explicit expressions for the screening energy and its gradient, *Journal of the Chemical Society Perkin Transactions*. 25 (1993) 799-805.
- [36] S. Wang, S. I. Sandler, Refinement of COSMO-SAC and the applications, *Industrial & Engineering Chemistry Research*. 47(2015) 1-15.
- [37] Y. Zhou, D. Xu, L. Zhang, Y. Ma, X. Ma, J. Gao, Y. Wang. Separation of thioglycolic acid from its aqueous solution by ionic liquids: Ionic liquids selection by the COSMO-SAC model and liquid-liquid phase equilibrium, *The Journal of Chemical Thermodynamics*. 118 (2018) 263-273.
- [38] Y. Zhou, D. Xu, L. Zhang, et al. Separation of thioglycolic acid from its aqueous solution by ionic liquids: Ionic liquids selection by the COSMO-SAC model and liquid-liquid phase equilibrium, *The Journal of Chemical Thermodynamics*. 118 (2018) 263-273.
- [39] C. M. Hsieh, S. I. Sandler, S. T. Lin, Improvements of COSMO-SAC for vapor-liquid and liquid-liquid equilibrium predictions, *Fluid Phase Equilibria*. 297 (2010) 90-97.
- [40] S. Wang, S. I. Sandler, Refinement of COSMO-SAC and the Applications, *Industrial & Engineering Chemistry Research*. 46 (2007) 7275-7288.
- [41] S. F. Boys, F. D. Bernardi, The calculation of small molecular interactions by the differences of separate total energies. Some procedures with reduced errors, *Mol. Phys.* 19 (1970) 553-566.
- [42] Aronica P G A, Fox S J, Verma C S. Comparison of Charge Derivation Methods Applied to Amino Acid Parameterization, *ACS Omega*. 3 (2018) 4664-4673.
- [43] Park J, Chun S, Bobik T A, et al. Molecular dynamics simulations of selective metabolite

- transport across the propanediol bacterial microcompartment shell, *The Journal of Physical Chemistry B*. 121 (2017) 8149-8154.
- [44] Wang J, Wolf R M, Caldwell J W, et al. Development and testing of a general amber force field, *Journal of computational chemistry*. 25 (2004) 1157-1174.
- [45] Ruscio J Z, Kohn J E, Ball K A, et al. The influence of protein dynamics on the success of computational enzyme design, *Journal of the American Chemical Society*. (2009) 14111-14115.
- [46] Bellesia G, Chundawat S P S, Langan P, et al. Probing the early events associated with liquid ammonia pretreatment of native crystalline cellulose, *The Journal of Physical Chemistry B*. 115 (2011) 9782-9788.
- [47] Gross A S, Bell A T, Chu J W. Entropy of cellulose dissolution in water and in the ionic liquid 1-butyl-3-methylimidazolium chloride, *Physical Chemistry Chemical Physics*. 14 (2012) 8425-8430.
- [48] Wen G, Geng X, Bai W, et al. Ternary liquid-liquid equilibria for systems containing (dimethyl carbonate or methyl acetate+ methanol+ 1-methylimidazole hydrogen sulfate) at 298.15 K and 318.15 K. *The Journal of Chemical Thermodynamics*. 121(2018) 49-54.
- [49] Zhu Z, Bai W, Qi P, et al. Liquid Liquid Equilibrium Data for the Separation of Acetone from n-Heptane Using Four Imidazolium-Based Ionic Liquids. *Journal of Chemical & Engineering Data*. 64(2019) 1202-1208.
- [50] Meindersma G W, Podt A, de Haan A B. Ternary liquid– liquid equilibria for mixtures of an aromatic+ an aliphatic hydrocarbon+ 4-methyl-N-butylpyridinium tetrafluoroborate[J]. *Journal of Chemical & Engineering Data*. (2006) 1814-1819.
- [51] Meindersma G W, Podt A J G, de Haan A B. Ternary liquid–liquid equilibria for mixtures of toluene+ n-heptane+ an ionic liquid[J]. *Fluid phase equilibria*. 247(2006) 158-168.
- [52] Ma Y, Xu X, Wen G, et al. Separation of Azeotropes Hexane+ Ethanol/1-Propanol by Ionic Liquid Extraction: Liquid–Liquid Phase Equilibrium Measurements and Thermodynamic Modeling[J]. *Journal of Chemical & Engineering Data*. (2007) 4296-4300.
- [53] Letcher T M, Deenadayalu N, Soko B, et al. Ternary liquid– liquid equilibria for mixtures of 1-methyl-3-octylimidazolium chloride+ an alkanol+ an alkane at 298.2 K and 1 bar[J].

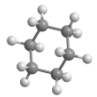

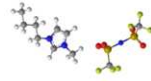
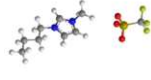

- Journal of Chemical & Engineering Data. 48(2003) 904-907.
- [54] Letcher T M, Deenadayalu N. Ternary liquid–liquid equilibria for mixtures of 1-methyl-3-octyl-imidazolium chloride+ benzene+ an alkane at T= 298.2 K and 1 atm[J]. The Journal of Chemical Thermodynamics. 35(2003) 67-76.
- [55] M. Mohsen-Nia, F. S. Mohammad Doulabi, Liquid–liquid equilibria for mixtures of (ethylene carbonate + aromatic hydrocarbon + cyclohexane), *Thermochimica Acta* 445 (2006) 82-85.
- [56] M. R. Mafra, M. A. Krahenbuhl, Liquid-Liquid Equilibrium of (Water + Acetone) with Cumene or α -Methylstyrene or Phenol at Temperatures of (323.15 and 333.15) K, *J. Chem. Eng. Data*. 51(2006) 753-756
- [57] R. S. Santiago, M. Aznar, Liquid–liquid equilibrium in ternary ionic liquid systems by UNIFAC: New volume, surface area and interaction parameters. Part II, *Fluid Phase Equilibr.* 303 (2011) 111-114.
- [58] T. Banerjee, M. K. Singh, R. K. Sahoo, A. Khanna, Volume, surface and UNIQUAC interaction parameters for imidazolium based ionic liquids via Polarizable Continuum Model, *Fluid Phase Equilibr.* 234 (2005) 64-76.
- [59] Zhu Z, Li X, Geng X, et al. Ternary Liquid–Liquid Equilibrium of Toluene+ Dimethyl Carbonate+ ILs at 298.15 K and Atmospheric Pressure[J]. *Journal of Chemical & Engineering Data*, 2019, 64(8) 3598-3605.

Table 1. Interaction energies between ILs and acetone.

System	E (hartree ^a)	E _{BSSE}	ΔE (kJ·mol ⁻¹)
acetone	-189.167163		
[BMIM]NTF ₂	-2251.239308		
[BMIM]OTF	-1375.750388		
[BMIM]N(CN) ₂	-654.334722		
[BMIM]NTF ₂ + acetone	-2443.900088	-0.001361	-73.581476
[BMIM]OTF + acetone	-1578.066862	-0.001472	-56.847552
[BMIM]N(CN) ₂ + acetone	-856.766519	-0.000785	-32.535705

^a1 hartree = 27.211 eV = 627.509 kcal·mol⁻¹ = 2625.753 kJ·mol⁻¹.

Table 2. Sources, CAS number, molar mass, purification, water contents by mass, w_w , and analysis method of the chemicals used in this work.

Chemical	Source	CAS number	Structure	Molecular formula	Molar mass/(g·mol ⁻¹)	Mass purity stated by supplier	w_w /10 ⁻⁶	Analysis method
cyclohexane	Tianjin Kermel Chemical Reagent Co., Ltd.	110-82-7		C ₆ H ₆	32.04	0.995 ^a		GC
acetone	Tianjin Kermel Chemical Reagent Co., Ltd.	67-64-1		CH ₃ COCH ₃	58.08	0.995 ^a		GC
[BMIM][NTF ₂]	Lanzhou Institute of Chemical Physics, Chinese Academy of Sciences.	174899-83-3		[C ₈ H ₁₅ N ₂][C ₂ F ₆ NO ₄ S ₂]	419.37	0.980 ^a	<500 ^a	
[BMIM][OTF]	Lanzhou Institute of Chemical Physics, Chinese Academy of Sciences.	174899-66-2		[C ₈ H ₁₅ N ₂][CF ₃ O ₃ S]	288.29	0.980 ^a	<500 ^a	
[BMIM][N(CN) ₂]	Lanzhou Institute of Chemical Physics, Chinese Academy of Sciences.	174501-64-5		[C ₈ H ₁₅ N ₂][C ₂ N ₃]	284.18	0.980 ^a	<500 ^a	

^aAnalysis by supplied

Table 3. Experimental LLE data on mole fraction x , distribution coefficient β and separation factor S for ternary systems of cyclohexane (1) + acetone (2) + ILs (3) at $T = 298.15$ K and $P = 101.325$ kPa^a.

		Lower phase		β	S
x_1	x_2	x_1	x_2		
cyclohexane (1) + acetone (2) + [BMIM][NTf ₂] (3) 298.15 K					
0.9729	0.0271	0.1261	0.4242	15.6531	120.7687
0.9480	0.0518	0.1266	0.5098	9.8417	73.6961
0.8939	0.1060	0.1273	0.6153	5.8047	40.7607
0.7863	0.2131	0.1714	0.6940	3.2567	14.9401
0.7643	0.2347	0.1954	0.6980	2.9740	11.6327
0.7129	0.2856	0.2144	0.6988	2.4468	8.1358
cyclohexane (1) + acetone (2) + [BMIM][OTF] (3) 298.15 K					
0.9824	0.0176	0.0835	0.2216	12.5909	148.1354
0.9620	0.0380	0.0767	0.3654	9.6158	120.6048
0.9334	0.0666	0.0776	0.4304	6.4625	77.7328
0.8782	0.1218	0.0798	0.5396	4.4302	48.7546
0.8370	0.1629	0.0920	0.6250	3.8367	34.9057
0.7691	0.2307	0.0918	0.6759	2.9298	24.5457
0.6987	0.3003	0.0999	0.7095	2.3626	16.5243
cyclohexane (1) + acetone (2) + [BMIM][N(CN) ₂] (3) 298.15 K					
0.9873	0.0127	0.0331	0.1359	10.7008	319.1809
0.9464	0.0535	0.0441	0.3157	5.9009	126.6359
0.8739	0.1259	0.0471	0.4699	3.7323	69.2501
0.8445	0.1552	0.0505	0.5568	3.5876	59.9951
0.7561	0.2436	0.0649	0.6190	2.5411	29.6038
0.6720	0.3275	0.0681	0.6764	2.0653	20.3805
0.6596	0.3398	0.0755	0.6834	2.0112	17.5705

^a Standard uncertainties u are $u(x_i) = 0.0119$, $u(T) = 0.05$ K, $u(p) = 1.5$ kPa, $u(m_i) = 0.0006$ g

$$u(m) = \frac{\text{MAE}}{\sqrt{3}}$$

Table 4. Binary interaction parameters Δg_{ij} , Δg_{ji} and nonrandomness factor α for NRTL model, binary interaction parameters Δu_{ij} and Δu_{ji} for UNIQUAC model and root-mean-square deviations, obtained from the experimental LLE data of studied ternary systems by NRTL and UNIQUAC models at $T = 298.15$ K and $P = 101.325$ kPa ^a.

$i-j$	Δg_{ij} (kJ·mol ⁻¹)	Δg_{ji} (kJ·mol ⁻¹)	$rmsd$	α
NRTL parameters				
cyclohexane (1) + acetone (2) + [BMIM][NTF ₂] (3) 298.15 K				
1-2	0.7477	1.1098	0.0023	0.20
1-3	12.5892	1.2939		
2-3	0.5699	-2.8837		
cyclohexane (1) + acetone (2) + [BMIM][OTF] (3) 298.15 K				
1-2	0.6162	0.9051	0.0029	0.20
1-3	9.2775	1.1348		
2-3	4.7574	-3.5896		
cyclohexane (1) + acetone (2) + [BMIM][N(CN) ₂] (3) 298.15 K				
1-2	0.4392	1.5175	0.0073	0.20
1-3	9.3129	1.8350		
2-3	4.2120	-2.3468		
UNIQUAC parameters				
cyclohexane (1) + acetone (2) + [BMIM][NTF ₂] (3) 298.15 K				
1-2	0.1489	1.7491	0.0124	
1-3	1.7937	0.4763		
2-3	-2.0992	1.1814		
cyclohexane (1) + acetone (2) + [BMIM][OTF] (3) 298.15 K				
1-2	1.0005	0.4829	0.0196	
1-3	0.3684	1.6628		
2-3	-2.4199	1.8183		
cyclohexane (1) + acetone (2) + [BMIM][N(CN) ₂] (3) 298.15 K				
1-2	2.6727	-0.2270	0.0180	
1-3	0.0852	3.1098		
2-3	-0.2886	1.1962		

^a Standard uncertainties u were $u(T) = 0.05$ K

Table 5. Volume (r_i) and surface area (q_i, q_i') of UNIQUAC equation

Component	r_i	q_i	q_i'
cyclohexane ^a	4.0464	3.2400	3.2400
acetone ^b	2.5730	2.3360	2.3360
[BMIM][NTf ₂] ^c	11.9640	9.7530	9.7530
[BMIM][OTF] ^d	12.4600	7.5180	7.5180
[BMIM][N(CN) ₂] ^e	22.6300	14.8600	14.8600

^aFrom reference [55]^bFrom reference [56]^cFrom reference [57]^dFrom reference [58]^eFrom reference [59]

1. The extraction process was studied by using quantum chemical calculation and RDF.
2. LLE data of cyclohexane + acetone + IL systems were measured.
3. The NRTL and UNIQUAC models were applied to correlate the studied system.

Journal Pre-proof

Declaration of interests

The authors declare that they have no known competing financial interests or personal relationships that could have appeared to influence the work reported in this paper.

The authors declare the following financial interests/personal relationships which may be considered as potential competing interests: